Published in final edited form as:
Ann Neurol. 2012 September ; 72(3): 395–405. doi:10.1002/ana.23606.

Apoptosis of oligodendrocytes in the CNS results in rapid focal demyelination

Andrew Caprariello[1], **Saisho Mangla**[2], **Robert H. Miller, Ph.D.**[2], and **Stephen M. Selkirk, M.D./Ph.D.**[3,4]

[1]Department of Physiology and Biophysics, Case Western Reserve School of Medicine, Cleveland Ohio

[2]Department of Neuroscience, Case Western Reserve School of Medicine, Cleveland Ohio

[3]Department of Neurology, Case Western Reserve School of Medicine, Cleveland, Ohio

[4]Spinal Cord Injury Division, Louis Stokes Cleveland Department of Veterans Affairs Medical Center, Cleveland Ohio

Abstract

Objective—Multiple sclerosis (MS) is a demyelinating disease of the central nervous system that presents with variable pathologies that may reflect different disease-causing mechanisms. Existing animal models of MS induce pathology using either local injection of gliotoxins or stimulation of the immune system with myelin-related peptides. In none of these models is the primary cellular target well characterized and although demyelination is a hallmark pathological feature in MS, it is unclear to what extent this reflects local oligodendrocyte loss. To unambiguously identify the effects of oligodendrocyte death in the absence of inflammatory stimulation, we developed a method for experimentally inducing programmed cell death selectively in mature oligodendrocytes and assessed the effects on demyelination, immunological stimulation and gliosis. The resulting pathology is discussed relative to observed MS pathologies.

Methods—Oligodendrocyte apoptosis was induced in the adult rat brain using a lentivirus to express experimentally-inducible caspase 9 (iCP9) cDNA under transcriptional control of the promoter for myelin basic protein (MBP), which is oligodendrocyte-specific. Activation of iCP9 was achieved by distal injection of a small molecule dimerizer into the lateral ventricle resulting in localized, acute oligodendrocyte apoptosis.

Results—Induced oligodendrocyte apoptosis resulted in rapid demyelination and robust, localized microglial activation in the absence of peripheral immune cell infiltration. Lesion borders showed layers of preserved and degraded myelin, while lesion cores were demyelinated but only partially cleared of myelin debris. This resulted in local proliferation and mobilization of the oligodendrocyte progenitor pool.

Interpretation—This approach provides a novel model to understand the pathological changes that follow from localized apoptosis of myelinating oligodendrocytes. It provides the first direct proof that initiation of apoptosis in oligodendrocytes is sufficient to cause rapid demyelination, gliosis and microglia response that result in lesions that share some pathological characteristics with a subset of MS lesions.

Corresponding author: Robert H. Miller, 2210 Circle Drive, SOM E721, Cleveland, OH 44106, 216.368.6269 (p), 216.368.4650 (f), Rhm3@case.edu.

INTRODUCTION

Multiple sclerosis (MS) is a demyelinating disease of the central nervous system (CNS) and is the leading cause of non-traumatic neurological disability in young adults. The cause of MS remains undefined although evidence supports an autoimmune mechanism by which dysregulation of myelin-specific T-lymphocytes causes CNS damage[1]. The precise repertoire of antigens in MS, however, remains unknown and while immune-targeted drug therapies may decrease relapse rate, they are less effective at preventing and do not reverse functional loss. A characteristic of MS is the presence of regions in the CNS that are devoid of myelin and oligodendrocytes but may retain abundant axons. The relative contribution of oligodendrocyte loss as a primary stimulus for demyelination is currently unclear.

A number of well-established animal models exist to study MS etiology and the relevant mechanisms of disease progression. Injection of glial-toxins such as lysolecithin, for example, produce demyelinating lesions with relative sparing of axons[2] allowing for spontaneous repair. While these models are useful for studying remyelination[3], their relevance to MS is complicated by a number of issues. Despite a systemic cell infiltrate and myelin antigen exposure, an auto-immune T-cell response is not propagated, even with repeated insults. Furthermore, the specificity of cell loss in these models is imprecise, astrocytes are damaged, and the blood brain barrier is transiently breached. These confounds complicate the interpretation of results as they relate to the initiation and progression of demyelination.

Experimental allergic encephalomyelitis (EAE) in mice is a well-studied model of MS. This model involves the induction of a CNS-specific immune response through systemic injection of CNS antigens and adjuvant. While EAE models some aspects of MS effectively, it is also limited. The use of a potent adjuvant to induce EAE may bypass essential components involved in MS initiation and progression. Furthermore, EAE can be induced with both myelin as well as non-myelin derivatives from astrocytes and other CNS cells[4–7] which may explain why agents that modify the immune response in EAE do not always modify the disease course in MS[8–9]. In none of the existing models is the primary cellular target well characterized. For example, gliotoxin injection damages astrocytes and endothelial cells in addition to oligodendrocytes and their precursors and EAE is often characterized by edema and inflammation rather than simply oligodendrocyte loss and frank demyelination, suggesting that MS is more complex than current animal models of the disease. Adding to the complexity of MS, the pathological courses between patients are often quite different. Comprehensive analyses of MS neuropathologies[10] between patients have led to the notion of pathologically-distinct categories of MS lesions[11, 12]. Two of four such MS subtypes implicate oligodendrocyte degeneration as a possible disease trigger, reminiscent of virus- or toxin-induced demyelination rather than autoimmunity. Likewise, studies of very early lesion formation in twelve MS patients who succumbed to an acute relapse revealed lesions containing extensive oligodendrocyte apoptosis and microglial activation in the absence of peripheral immune cell infiltration[13]. A separate study of fourteen patients with acute MS exacerbations showed Baló-like alternating rims of demyelination and preserved myelination at the lesion borders in a manner previously linked to oligodendrocyte loss[14, 15]. Together, these data support the notion that oligodendrocyte loss may be a contributing factor in the initiation of subsets of MS lesions.

To determine whether the induction of oligodendrocyte apoptosis is sufficient to drive demyelination in the absence of inflammation or additional local insults we developed a novel model of experimentally-induced apoptosis in mature oligodendrocytes. Experimental apoptosis is achieved through small-molecule dimerization of an engineered, inducible caspase-9 (iCP9) transgene delivered to the corpus callosum using a lentivirus. A cell-

specific promoter sequence driving iCP9 expression restricts cell death in the CNS to oligodendrocytes. Following induced oligodendrocyte apoptosis, rapid demyelination ensued, triggering robust, localized microglial activation in the absence of peripheral T-lymphocytes. The iCP9 model represents a potential tool for understanding the response of the adult CNS to selective oligodendrocyte apoptosis and indicates that such cell loss is sufficient to stimulate demyelination and a rapid endogenous microglial response.

Methods

Cloning of iCP9 lentiviral vector

The first generation, self-inactivating lentiviral vector pLpMG (gift from Dr. Stanton Gerson, CWRU) was modified by insertion of a fragment of the rat Myelin Basic Protein promoter (pMBP)[17]. The resulting vector, pLpMBPxMG, was further modified by ligation of the iCP9 cDNA sequence downstream of pMBP (Fig 1A). The vector, pLpMBP(iCP9)MG, was used to generate high titer, replication incompetent lentivirus[18]. The same vector contained the sequence for GFP under transcriptional control of a viral promoter, allowing for identification of infected cells before and after CID administration. Viral titer was determined against 293T cells followed by FACS analysis for GFP expression. All titers used *in vivo* were at least 10^9 colony-forming units per ml. The iCP9 cDNA was kindly provided by Dr. David Spencer (Baylor University). It was engineered by linking the caspase 9 cDNA sequence, after removal of the caspase recruitment domain (CARD), to a FK506 binding protein (FKBP) sequence (GenBank AH002818). The absence of the CARD sequence prevents physiologic protein dimerization and cell death[16]. Fusion to the FKBP sequence enables experimental activation with an FK506 analog, termed chemical inducer of dimerization (CID, Fig 1B). The CID was altered to prevent interaction with endogenous FKBPs (Dalton Pharmaceuticals).

In vitro application of lentiviral vector and immunocytochemistry

Primary rat cortical cultures were established as previously described[19]. Cultures were plated on poly-L-lysine-coated coverslips (1×10^4 cells per coverslip) and grown in defined media for three days after which lentivirus was added. Twenty-four hours later 10nm CID was added. Control cultures were infected with virus but not exposed to CID. Cultures were fixed and labeled with antibodies to identify specific cell types. The proportions of the different cell types that were GFP^+ were counted from ten randomly selected fields taken from at least 2 different coverslips from 3 separate preparations and the results compared between CID treated and control cultures.

For immunocytochemistry, cells were fixed at room temperature with 4% PFA for 20 minutes followed by incubation in primary antibody (A2B5, 1:2; O4/O1, 1:4; MBP [Covance SMI99], 1:500; GFAP [Dako], 1:500) in 5% NGS/0.3% triton for 30 min at RT followed by secondary antibody (Alexa 594 [Invitrogen], 1:500) for 30 minutes at RT. Labeling with mAbs A2B5, O4 and O1 was performed on live cultures that were subsequently fixed in 4% PFA. Cultures were mounted using Vectashield with DAPI and examined on a Leica DM5500B upright microscope equipped with epiflouresence.

Brain injections of lentiviral vector and CID

All animal procedures were conducted in accordance with NIH guidelines and were reviewed and approved by animal subcommittees at both the Cleveland VA Medical Center and CWRU. Under a BSL2 hood, lentivirus was injected into the corpus callosum of anesthetized rats using stereotaxic guidance as previously described[20]. One week later, CID was injected into the ipsilateral ventricle distal to the initial site of injection. CID was resuspended in 100% ethanol to a concentration of 1mM and diluted 1:1000 in PBS. A full

week was allowed between the initial injection of lentivirus and injection of CID in order to provide sufficient time for any inflammatory response to return to baseline and for robust integration of the iCP9 construct into the target tissue.

Tissue processing and analysis

One and seven days post-CID, rats were sacrificed via transcardial perfusion with 0.9% saline followed by 4% PFA. Brains were removed, placed in 30% sucrose overnight, embedded in OCT, and sectioned on a cryostat at 20 μm. Fluorescent microscopy was used to visualize infected cells. Myelin loss was identified using either Black-Gold histochemistry (Histochem, Jefferson AR) or MBP immunostaining. For immunohistochemistry, sections were treated as described above for cultures except incubation in the primary antibody was overnight at 4°C. Primary antibodies used were GFAP, A2B5, O4, O1, Olig2 (Chemicon, 1:500), GFP (Invitrogen, 1:500), CC1 (Oncogene, 1:250), cCP3 (Cell Signaling, 1:100), and Ki67 (BD Pharmogen, 1:250). For double-labeling experiments, primary antibodies were mixed together and applied to tissue sections as a mixed solution for the overnight incubation period.

Tissue Cell Counts

Cell quantification in the in vivo experiments were generated using blinded counts of immunolabeled cells in 5 consecutive, non-overlapping, white matter fields beginning with the medial aspect of the subventricular zone and proceeding laterally. The same area of tissue (approximately 0.9–1.5 mm^2) was analyzed in at least 2 sections of 4 or 5 rat brains per experiment. Statistical significance was assessed using an unpaired Student's T-test.

Results

CID selectively decreases GFP^+ oligodendrocytes in primary brain cultures

To determine the efficacy and specificity of the iCP9 system for initiating oligodendrocyte death, studies were conducted using primary neonatal rat brain cultures. In these experiments, cultures were infected with lentivirus carrying the iCP9 construct (pLpMBP(iCP9)MG), exposed to CID for twenty-four hours, and analyzed for cell death by comparing the relative numbers of different neural cell types in treated versus untreated cultures. After exposure to virus, routinely 60– 70% of cells were infected and this was proportional to the amount of virus that was added to the culture. The cells appeared morphologically normal and total cell counts of virally-infected versus uninfected cultures were similar, indicating that neither virus alone nor inappropriate iCP9 activation induced cell loss. After CID exposure, the relative proportion of MBP^+ cells infected with virus (MBP^+/GFP^+) was significantly reduced compared to control cultures. This reduction was specific to mature oligodendrocytes ($O1^+$ and MBP^+) as the numbers of GFP^+, virus-infected $A2B5^+$ oligodendrocyte progenitor cells, $O4^+$ immature oligodendrocytes, or $GFAP^+$ astrocytes were not statistically different in CID-treated compared to control cultures (Fig 2). The few MBP^+/GFP^+ cells remaining in the experimental cultures displayed hallmark signs of apoptosis including nuclear condensation, membrane blebbing, and truncated cell processes. By contrast the other GFP^+ cell types exposed to CID were morphologically indistinguishable from cells in control cultures. These data validate the efficacy and specificity of CID-induced apoptosis of mature oligodendrocytes.

CID decreases GFP^+ oligodendrocytes in the adult rat brain

To determine the potential of CID to induce oligodendrocyte apoptosis in vivo, lentivirus containing the MBP-iCP9 construct was injected into the rat corpus callosum. One week later, CID was delivered distally to the ipsilateral ventricle and after a further twenty-four

hours the proportion of GFP^+ cells expressing CC1, a marker of mature oligodendrocytes, was compared to vehicle-injected, control animals. In control animals, $CC1^+$ oligodendrocytes represented approximately 45% of all infected cells (n=5), which constituted approximately 20% of the total number of $CC1^+$ oligodendrocytes in the targeted region of the corpus callosum (Fig 3). By contrast, following injection of the cross-linking CID agent, the average number of $CC1^+$ oligodendrocytes per 20× field decreased significantly (control 162+/− 1: experimental 86+/− 4) compared to either the contralateral corpus callosum or to a separate vehicle-treated control animal (Fig 4). The relative loss of $CC1^+$ oligodendrocytes was closely matched by the loss of $CC1^+/GFP^+$ virally-infected oligodendrocytes (control 44+/− 10% : experimental 20+/− 1%). These data were consistent with the in vitro studies, which together indicate the capability of the MBP-iCP9 construct to selectively ablate oligodendrocytes. To show that ablation occurred secondary to induced apoptosis, immunostaining was conducted using both cleaved Caspase 3, the downstream effector of Caspase 9, and TUNEL, which identifies nicked-end DNA in apoptotic cells. The vast majority of $CC1^+$ oligodendrocytes in the lesion were also both cleaved caspase 3^+ and $TUNEL^+$ following CID treatment consistent with the induction of apoptosis (Fig 4).

To assess the specificity of induced apoptosis, tissue sections from control and CID treated animals were probed with cell-specific antibodies to astrocytes, microglia, and axonal neurofilaments. Quantification of $GFAP^+$ astrocytes in the lesion area showed no significant differences in CID-treated animals compared to either the contralateral corpus callosum or to vehicle-treated control animals (control 110+/− 7 : experimental 120+/− 2) (Fig 5). Similarly, no discernible changes were found in axonal neurofilaments by confocal microscopy, while the number of $IBA1^+$ microglia significantly increased (control 50 +/− 1 : experimental 110 +/− 2). These data verify the oligodendrocyte-specificity of CID-mediated death.

Oligodendrocyte death increases the number of proliferating OPCs

In models where demyelination is induced in a less cell-type-specific manner, insults are often associated with a local increase in the proliferation of progenitor cells. To determine the extent and nature of cell proliferation following induced oligodendrocyte apoptosis, sections through the lesion and corresponding control areas were labeled with antibodies to Ki67, which identifies proliferating cells. In vehicle-injected control animals a low level of proliferation occurred in the virally-infected regions expressing GFP (193+/−15), which was markedly increased in animals that received CID injections (353+/−30) (Fig 6). To assess the proportion of the proliferating cells that were of the oligodendrocyte lineage, sections were double labeled with antibodies against the transcription factor Olig2. While the proportion of proliferative Olig2-negative cells showed some increase (152+/− 41 : 205 +/− 64), the larger increase in proliferating cells was attributable to the $Olig2^+$ population (40+/− 12 : 150+/− 37). The highest density of proliferating cells was located adjacent to the subventricular zone and the enhanced cell proliferation was absent from the contralateral hemisphere of experimental animals. These data suggest that the induction of apoptosis in mature oligodendrocytes is sufficient to stimulate a proliferative response in local OPCs.

Oligodendrocyte apoptosis leads to rapid myelin loss

Induced oligodendrocyte apoptosis resulted in rapid, localized myelin disturbances. Twenty-four hours after injection of CID, an area of demyelination was present that directly correlated with the region containing a markedly decreased number of GFP^+ cells, whereas the surrounding regions appeared normal. The loss of myelin was identified using a number of histological myelin assays. Lesions contained Black-Gold-positive fragments of degraded myelin and an absence of MBP immunofluorescence compared to controls (Fig 7).

To rule out the possibility that myelin loss was caused by either the virus or the cross-linking CID agent, control animals were injected with a different lentivirus designed to target astrocytes in which iCP9 was inserted downstream of an astrocyte-specific GFAP promoter (pLpGFAP(iCP9)MG). Following CID injection into rats expressing pLpGFAP(iCP9)MG, there were no signs of demyelination up to seven days after CID exposure despite evidence of functional loss of astrocytes using an IgG blood-brain barrier integrity assay (Fig 7). In additional controls, animals were injected with an empty vector lacking the iCP9 sequence (pLpMBP(X)MG) and subsequently treated with CID. Although strong GFP labeling indicated successful viral delivery, the myelin appeared healthy and undisturbed despite exposure to both virus and CID (data not shown). Likewise, injections of CID alone in the absence of virus did not cause noticeable cytotoxicity or demyelination.

Further evidence of demyelination came from ultrastructural analyses of the lesions, which revealed demyelinated axons and glial processes interspersed with intact myelinated axons. This data likely reflects the fact that only 20–30% of the total number of oligodendrocytes expressed iCP9 and were therefore susceptible to CID-mediated death. Localized oligodendrocyte death resulted in a characteristic pattern in which axons were myelinated on one internode but demyelinated on adjacent segments (Fig 8). Accordingly, the interface of myelinated and demyelinated regions was usually seen at a node. In thin sections stained with Toluidine Blue, the lesion borders contained alternating patterns of preserved and degraded myelin, a pattern of demyelination previously linked to oligodendrocyte loss[14, 15].

Apoptosis-mediated demyelination coincides with a robust microglia response and delayed T-cell infiltration

One unexpected finding from these studies was the remarkably rapid loss of myelin basic protein immunofluorescence from the lesion area. One potential mechanism of myelin clearance is the activation of phagocytic cells. Consistent with this possibility, cell counts of microglia/macrophages labeled with anti-IBA1 antibodies showed a significant increase in cell number and an obvious morphological change from a resting to an activated state. Further, GFP^+ fragments were identified within $IBA1^+$ microglia suggesting phagocytosis of degraded myelin (Fig 9). This finding was confirmed in thin sections stained with Toluidine Blue, which clearly demonstrated myelin-containing phagocytic cells. However, nearby Black-Gold-positive myelin debris indicated incomplete phagocytosis after twenty-four hours. Although iCP9-mediated demyelination triggered rapid and robust microglial activation within and surrounding the areas of demyelination, early lesions were devoid of blood-borne $CD3^+$ T-cells. One week later, T-cells appeared and microglia were still activated yet myelin debris persisted. Together these data suggest that localized induction of oligodendrocyte apoptosis results in rapid demyelination that is accompanied first by localized activation of CNS-resident microglia/macrophages and then delayed infiltration of blood-borne $CD3^+$ T-cells.

Discussion

In this study we demonstrate a unique system to selectively ablate oligodendrocytes in a focal manner. The induced apoptotic cascade, which is limited to adult oligodendrocytes, produces a focal demyelinated lesion without the administration of exogenous toxins into the CNS or the systemic administration of an antigen and adjuvant. The induction of oligodendrocyte apoptosis results in rapid local demyelination and the localized activation of microglial cells. The infiltration of immune cells is delayed and follows rather than precedes demyelination in this model.

Established animal models of MS have provided the framework for understanding important aspects of the disease. Localized injection of toxins such as lysolecithin or ethidium bromide

are useful for studying demyelination and remyelination[22] under controlled, reproducible conditions, while EAE has utility for understanding mechanisms of immune cell infiltration and immune-mediated demyelination. Our system offers a new perspective to assess the induction of demyelination resulting from oligodendrocyte death and models an additional component that may be important in the generation of MS lesions. In the iCP9 model, oligodendrocyte death is experimentally induced by short-circuiting an existing cell death pathway that has been reported in early MS lesions but whose significance for MS pathogenesis remains unknown[10–15, 23].

To our knowledge, this is the first report of a model in which oligodendrocytes are eliminated in both a physiological- and potentially disease-relevant manner. While the current studies are restricted to analysis of oligodendrocyte loss in the adult corpus callosum it is potentially applicable to the other regions of the adult CNS as well as during development. Such studies may reveal important regional differences in the response to oligodendrocyte death. The primary restriction in such studies is the limits of diffusion of the cross-linker from its site of injection to iCP9-expressing oligodendrocytes. The current studies suggest CID needs only to be administered to a nearby CSF-access point, such as the cisterna magna, the lateral ventricles, or the vitreous of the eye for near-complete coverage of the spinal cord, brain, or optic nerve, respectively.

An important aspect of the MBP-iCP9 model is that allows for the study of demyelinating events in the absence of a systemic inflammatory response. This may have clinical relevance since it has been suggested that some early MS lesions are characterized by extensive oligodendrocyte apoptosis prior to systemic inflammatory cell infiltration[13, 24–25]. Consistent with this hypothesis, iCP9-mediated lesion borders contained alternating patterns of demyelination and preserved myelination, a pattern similar to that seen in Baló's concentric sclerosis, a disease variant of MS[14, 15], and in Type III patterns of MS that may result from oligodendrocyte dystrophy[12].

The induction of oligodendrocyte apoptosis and subsequent microglial activation is sufficient to stimulate local proliferation of OPCs. A comparison of proliferating $Ki67^{+}$ cells in control and experimental animals demonstrated a selective proliferative response in OPCs, the majority of which were located adjacent to the subventricular zone. The low level of OPC proliferation seen in the absence of demyelination likely reflects the continuous generation of oligodendrocytes in the adult corpus callosum[37]. The stimuli responsible for enhanced OPC proliferation is unknown, however it has been reported in other models of demyelination and remeylination as well as in MS lesions[38s]. One attractive hypothesis is this reflects an attempt at endogenous repair, however in slice preparations[39] and in chronic MS lesions[40] loss of mature oligodendrocytes often fails to stimulate effective myelin repair.

The activation of CNS microglia occurs in in response to cellular debris, acute injury and chronic disease[26–29]. Following oligodendrocyte apoptosis, a rapid microglia/macrophage response was seen as early as twenty-four hours later. Given this robust response and the absence of T-cells at this early time point, it appears the initial response to oligodendrocyte apoptosis is one of local scavenging rather than a systemic inflammatory reaction. A similar robust microglia response has been identified in acute MS lesions[24]. In these neuropathological specimens, activated microglia were found primarily in pre-phagocytic regions that were actively demyelinating but generally devoid of T and B cells. In contrast, in areas of active phagocytosis or repair, microglia were less common and T and B cells predominated.

The observation that myelin components are rapidly cleared after cell death contrasts with recent reports of global oligodendrocytes ablation using diphtheria toxin (DT). For example,

a lack of myelin removal after DT-mediated oligodendrocyte death was observed [30]. Microglia/macrophage activation occurred around vacuoles that developed from the splitting of the myelin sheath lamellae but not until four weeks after oligodendrocyte death. Similarly, a 4–5 week delay in microglial activation was seen [31] even though oligodendrocytes were ablated by seven days of treatment. Thus, following DT-mediated oligodendrocyte cell death, myelin sheaths appear to remain intact despite being disconnected from a viable cell body. The basis for the different rate of myelin clearance is unclear, however we propose the mechanism of cell death dictates the response of the local environment to oligodendrocyte death. In the iCP9 model, oligodendrocyte death is restricted to an apoptotic pathway unassociated with significant cellular stress prior to death. By contrast, DT blocks protein synthesis and in doing so, presumably generates a prolonged period of pre-death cellular stress and initiation of pro-inflammatory cell death. Normal apoptotic cell death involves the expression and release of molecules that activate a local scavenging response for rapid cellular removal[32]. For example, the externalization of phosphatidyleserine (PS), the release of intracellular metabolites (e.g. ATP), chromatin binding proteins and nucleotides have all been shown to mediate microglia activation[33, 34]. Apoptotic cells also suppress the secretion of pro-inflammatory cytokines[35] to promote immunological tolerance, which may explain why peripheral T-cells were absent from early iCP9 lesions. In the DT model, by contrast, cellular responses to stress are variable and distinct from the apoptotic pathway[32]. As cellular stress persists and RNA translation is prevented by diphtheria toxin, factors generated by cells are likely limited, and typical pro-phagocytic signals and pro-inflammatory molecules may not be elicited to a degree that activates clearance of myelin.

One factor common between previous models of demyelination is the robust systemic inflammatory infiltrate that accompanies the demyelinating event. In the current model, however, the systemic inflammatory response appears limited despite focal oligodendrocyte death. Given the absence of a systemic immune infiltrate in some pre-phagocytic MS lesions, the iCP9 system may provide a tool for modeling a novel aspect of disease pathogenesis. Moving forward, it will be important to differentiate pathogenic mechanisms attributable to the immune system versus potential cell degeneration in the CNS[36].

Summary

A model of inducible oligodendrocyte apoptosis allows for the spatial and temporal characterization of the adult CNS responses to the induction of apoptosis in mature oligodendrocytes. The current data demonstrates rapid and robust demyelination that is accompanied by local microglial activation but precedes extensive immune cell infiltration. The loss of mature oligodendrocytes is associated with a selective increase in the local proliferation of OPCs suggesting a dynamic regulation of oligodendrocyte numbers in the adult. These results may have direct clinical relevance since it has been proposed that a subtype of MS is characterized by oligodendrocyte dystrophy.

Acknowledgments

This study was supported by the Myelin Repair Foundation (R.H.M), the National Institutes of Health Grant NS030800 (R.H.M) and a VA Career Development Award-2 (S.M.S).

References

1. Martin R, McFarland HF, McFarlin DE. Immunological aspects of demyelinating diseases. Annu Rev Immunol. 1992; 10:153–187. [PubMed: 1375472]

2. Wang Y, Wu C, Caprariello AV, et al. In vivo quantification of myelin changes in the vertebrate nervous system. The Journal of neuroscience : the official journal of the Society for Neuroscience. 2009 Nov 18; 29(46):14663–14669. [PubMed: 19923299]
3. Blakemore WF, Franklin RJ. Remyelination in experimental models of toxin-induced demyelination. Curr Top Microbiol Immunol. 2008; 318:193–212. [PubMed: 18219819]
4. Waksman BH, Porter H, Lees MD, et al. A study of the chemical nature of components of bovine white matter effective in producing allergic encephalomyelitis in the rabbit. J Exp Med. 1954 Nov 1; 100(5):451–471. [PubMed: 13211907]
5. Linington C, Lassmann H, Ozawa K, et al. Cell adhesion molecules of the immunoglobulin supergene family as tissue-specific autoantigens: induction of experimental allergic neuritis (EAN) by P0 protein-specific T cell lines. Eur J Immunol. 1992 Jul; 22(7):1813–1817. [PubMed: 1378018]
6. Linington C, Berger T, Perry L, et al. T cells specific for the myelin oligodendrocyte glycoprotein mediate an unusual autoimmune inflammatory response in the central nervous system. Eur J Immunol. 1993 Jun; 23(6):1364–1372. [PubMed: 7684687]
7. Wekerle H, Kojima K, Lannes-Vieira J, et al. Animal models. Annals of neurology. 1994; 36(Suppl):S47–S53. [PubMed: 7517126]
8. van Oosten BW, Lai M, Hodgkinson S, et al. Treatment of multiple sclerosis with the monoclonal anti-CD4 antibody cM-T412: results of a randomized, double-blind, placebo-controlled, MR-monitored phase II trial. Neurology. 1997 Aug; 49(2):351–357. [PubMed: 9270561]
9. Sriram S, Steiner I. Experimental allergic encephalomyelitis: a misleading model of multiple sclerosis. Annals of neurology. 2005 Dec; 58(6):939–945. [PubMed: 16315280]
10. Breij EC, Brink BP, Veerhuis R, et al. Homogeneity of active demyelinating lesions in established multiple sclerosis. Annals of neurology. 2008 Jan; 63(1):16–25. [PubMed: 18232012]
11. Lucchinetti C, Bruck W, Parisi J, et al. A quantitative analysis of oligodendrocytes in multiple sclerosis lesions. A study of 113 cases. Brain. 1999 Dec; 122(Pt 12):2279–2295. [PubMed: 10581222]
12. Lucchinetti C, Bruck W, Parisi J, et al. Heterogeneity of multiple sclerosis lesions: implications for the pathogenesis of demyelination. Annals of neurology. 2000 Jun; 47(6):707–717. [PubMed: 10852536]
13. Barnett MH, Prineas JW. Relapsing and remitting multiple sclerosis: pathology of the newly forming lesion. Annals of neurology. 2004 Apr; 55(4):458–468. [PubMed: 15048884]
14. Yao DL, Webster HD, Hudson LD, et al. Concentric sclerosis (Balo): morphometric and in situ hybridization study of lesions in six patients. Annals of neurology. 1994 Jan; 35(1):18–30. [PubMed: 8285587]
15. Stadelmann C, Ludwin S, Tabira T, et al. Tissue preconditioning may explain concentric lesions in Balo's type of multiple sclerosis. Brain. 2005 May; 128(Pt 5):979–987. [PubMed: 15774507]
16. Straathof KC, Pule MA, Yotnda P, et al. An inducible caspase 9 safety switch for T-cell therapy. Blood. 2005 Jun 1; 105(11):4247–4254. [PubMed: 15728125]
17. Goujet-Zalc C, Babinet C, Monge M, et al. The proximal region of the MBP gene promoter is sufficient to induce oligodendroglial-specific expression in transgenic mice. Eur J Neurosci. 1993 Jun 1; 5(6):624–632. [PubMed: 7505168]
18. Coleman JE, Huentelman MJ, Kasparov S, et al. Efficient large-scale production and concentration of HIV-1-based lentiviral vectors for use in vivo. Physiol Genomics. 2003 Feb 6; 12(3):221–228. [PubMed: 12488511]
19. Fyffe-Maricich SL, Karlo JC, Landreth GE, et al. The ERK2 mitogen-activated protein kinase regulates the timing of oligodendrocyte differentiation. The Journal of neuroscience : the official journal of the Society for Neuroscience. 2011 Jan 19; 31(3):843–850. [PubMed: 21248107]
20. Caprariello AV, Miller RH, Selkirk SM. Foamy virus as a gene transfer vector to the central nervous system. Gene therapy. 2009 Mar; 16(3):448–452. [PubMed: 19052632]
21. Barnett MH, Sutton I. The pathology of multiple sclerosis: a paradigm shift. Curr Opin Neurol. 2006 Jun; 19(3):242–247. [PubMed: 16702829]
22. Matsushima GK, Morell P. The neurotoxicant, cuprizone, as a model to study demyelination and remyelination in the central nervous system. Brain Pathol. 2001 Jan; 11(1):107–116. [PubMed: 11145196]

23. Artemiadis AK, Anagnostouli MC. Apoptosis of oligodendrocytes and post-translational modifications of myelin basic protein in multiple sclerosis: possible role for the early stages of multiple sclerosis. Eur Neurol. 2010; 63(2):65–72. [PubMed: 20068323]
24. Henderson AP, Barnett MH, Parratt JD, et al. Multiple sclerosis: distribution of inflammatory cells in newly forming lesions. Annals of neurology. 2009 Dec; 66(6):739–753. [PubMed: 20035511]
25. Barnett MH, Parratt JD, Pollard JD, et al. MS: is it one disease? Int MS J. 2009 Jun; 16(2):57–65. [PubMed: 19671369]
26. Neumann H, Kotter MR, Franklin RJ. Debris clearance by microglia: an essential link between degeneration and regeneration. Brain. 2009 Feb; 132(Pt 2):288–295. [PubMed: 18567623]
27. Block ML, Zecca L, Hong JS. Microglia-mediated neurotoxicity: uncovering the molecular mechanisms. Nat Rev Neurosci. 2007 Jan; 8(1):57–69. [PubMed: 17180163]
28. Chen J, Zhou Y, Mueller-Steiner S, et al. SIRT1 protects against microglia-dependent amyloid-beta toxicity through inhibiting NF-kappaB signaling. J Biol Chem. 2005 Dec 2; 280(48):40364–40374. [PubMed: 16183991]
29. Streit WJ. Microglia and neuroprotection: implications for Alzheimer's disease. Brain Res Brain Res Rev. 2005 Apr; 48(2):234–239. [PubMed: 15850662]
30. Pohl HB, Porcheri C, Mueggler T, et al. Genetically induced adult oligodendrocyte cell death is associated with poor myelin clearance, reduced remyelination, and axonal damage. The Journal of neuroscience : the official journal of the Society for Neuroscience. 2011 Jan 19; 31(3):1069–1080. [PubMed: 21248132]
31. Traka M, Arasi K, Avila RL, et al. A genetic mouse model of adult-onset, pervasive central nervous system demyelination with robust remyelination. Brain. 2010 Oct; 133(10):3017–3029. [PubMed: 20851998]
32. Zitvogel L, Kepp O, Kroemer G. Decoding cell death signals in inflammation and immunity. Cell. 2010 Mar 19; 140(6):798–804. [PubMed: 20303871]
33. Ghiringhelli F, Apetoh L, Tesniere A, et al. Activation of the NLRP3 inflammasome in dendritic cells induces IL-1beta-dependent adaptive immunity against tumors. Nat Med. 2009 Oct; 15(10): 1170–1178. [PubMed: 19767732]
34. Elliott MR, Chekeni FB, Trampont PC, et al. Nucleotides released by apoptotic cells act as a find-me signal to promote phagocytic clearance. Nature. 2009 Sep 10; 461(7261):282–286. [PubMed: 19741708]
35. Ronchetti A, Rovere P, Iezzi G, et al. Immunogenicity of apoptotic cells in vivo: role of antigen load, antigen-presenting cells, and cytokines. J Immunol. 1999 Jul 1; 163(1):130–136. [PubMed: 10384108]
36. Tsutsui S, Stys PK. Degeneration versus autoimmunity in multiple sclerosis. Annals of neurology. 2009 Dec; 66(6):711–713. [PubMed: 20033985]
37. Psachoulia K, Jamen F, Young KM, Richardson WD. Cell cycle dynamics of NG2 cells in the postnatal and ageing brain. Neuron Glia Biol. 2009 Nov; 5(3–4):57–67. [PubMed: 20346197]
38. Woodruff RH, Fruttiger M, Richardson WD, Franklin RJ. Platelet-derived growth factor regulates oligodendrocyte progenitor numbers in adult CNS and their response following CNS demyelination. Mol Cell Neurosci. 2004; 25(2):252–262. [PubMed: 15019942]
39. Yang Y, Lewis R, Miller RH. Interactions between oligodendrocyte precursors control the onset of CNS myelination. Dev Biol. 2011; 350(1):127–138. [PubMed: 21144846]
40. Patrikios P, Stadelmann C, Kutzelnigg A, et al. Remyelination is extensive in a subset of multiple sclerosis patients. Brain. 2006; 129(12):3165–3172. [PubMed: 16921173]

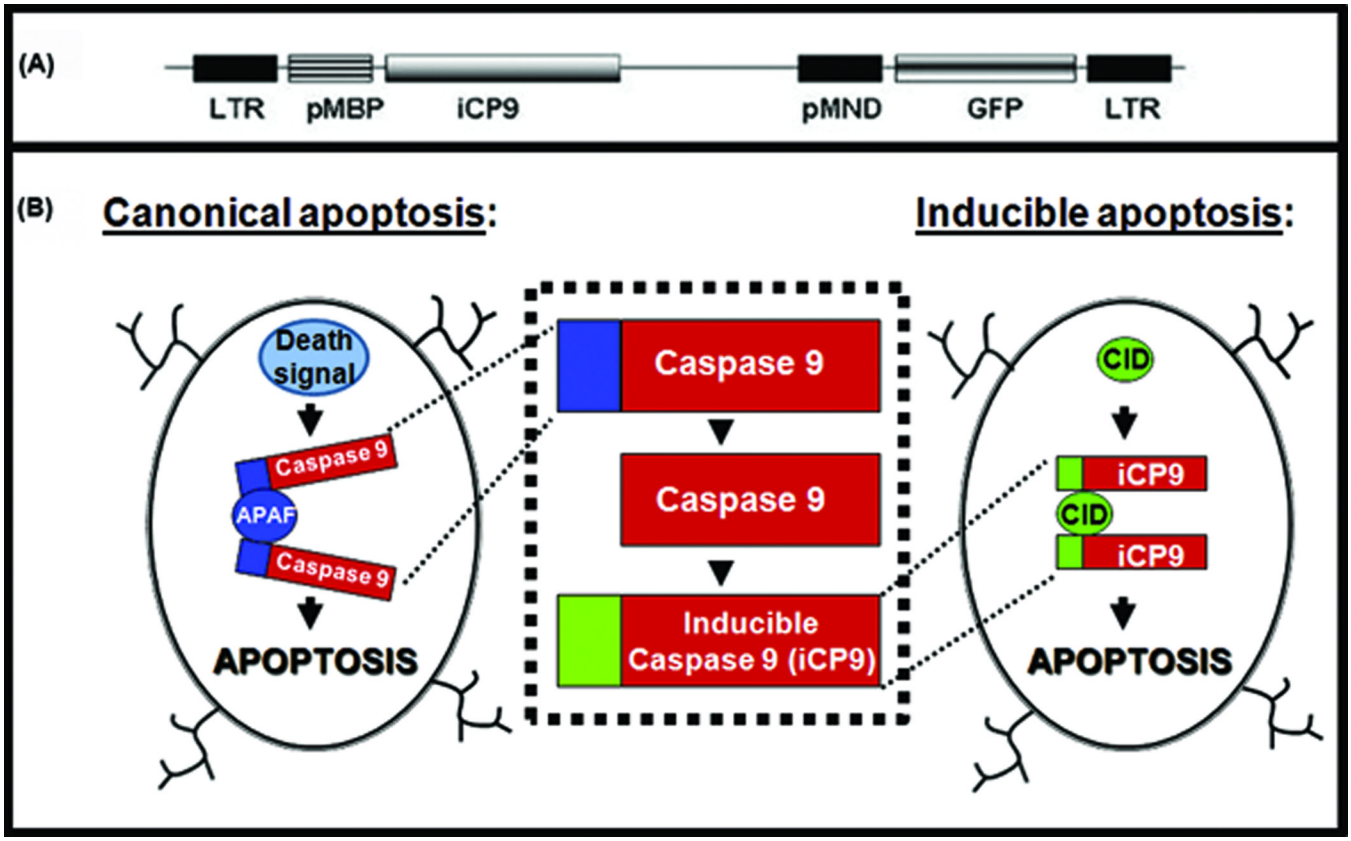

Figure 1.

Diagrammatic representation of the lentiviral construct engineered to induce oligodendrocyte apoptosis. (**A**) Schematic of the viral construct in which an oligodendrocyte-specific promoter sequence (pMBP) drives expression of a suicide gene that is a chemically-inducible analogue of the endogenous Caspase 9 (iCP9). The reporter GFP was expressed downstream driven from a constitutive viral promoter. (**B**) During canonical apoptosis Caspase 9 dimerizes through binding to APAF-1 to initiate the apoptotic cascade while in the inducible model the N-terminal domain of Caspase 9 (blue) was modified with removal of the APAF-1 binding site and replacement with a CID binding domain to allow chemically-induced dimerization (CID, green). LTR = long terminal repeat; pMBP = promoter for myelin basic protein; pMND = promoter from modified murine leukemia virus; GFP = green fluorescent protein; APAF = apoptotic protease activating factor.

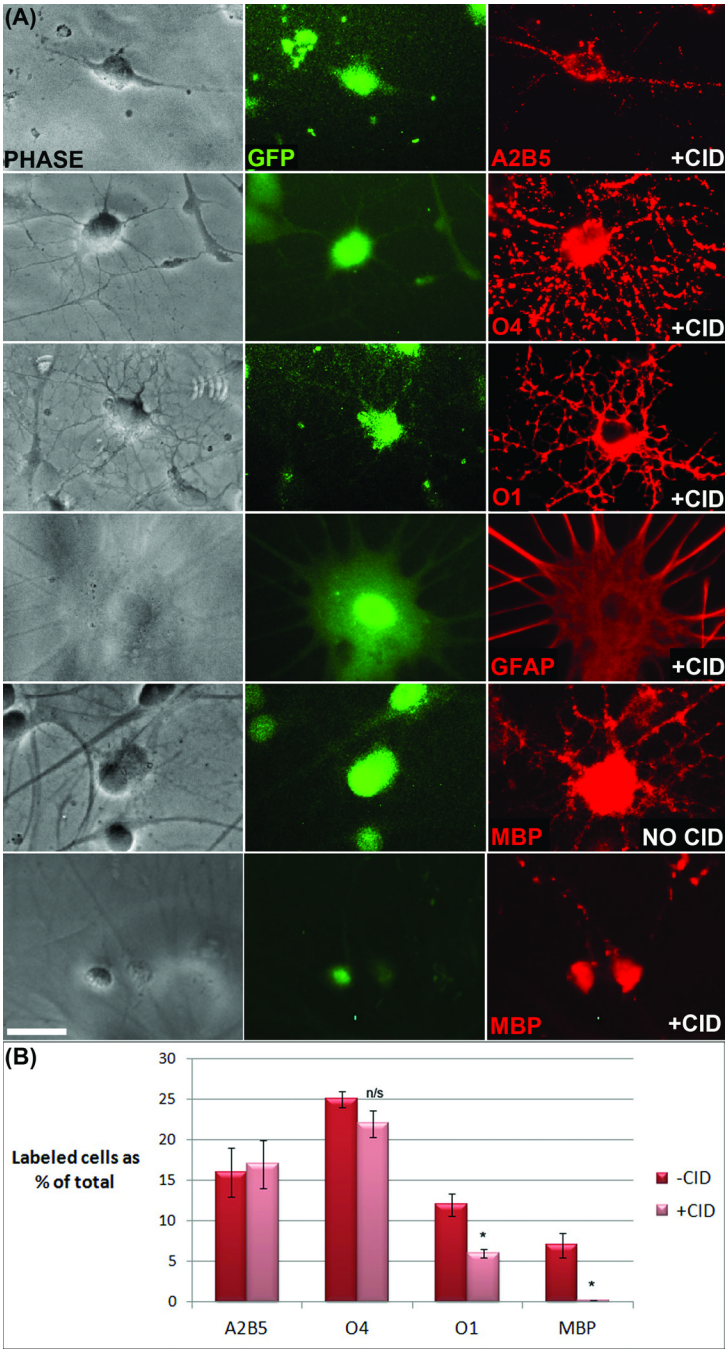

Figure 2.

Viral delivery of iCP9 and subsequent exposure to CID resulted in selective ablation of mature oligodendrocytes in vitro. (**A**) Primary neonatal rat cultures labeled with cell type-specific antibodies indicated that astrocytes, oligodendrocytes and their precursors were effectively transduced by the virus and that viral transduction in the absence of CID has no effect on cell survival. Addition of CID had no effect on the survival of transduced, GFP-expressing A2B5$^+$ oligodendrocyte precursor cells, O4$^+$ immature oligodendrocytes, or GFAP$^+$ astrocytes but significantly decreased the number of MBP$^+$ mature oligodendrocytes in the culture. (**B**) Quantification of the relative proportion of oligodendrocyte lineage cells

within the GFP^+ population in parallel cultures before and after CID demonstrated that cell death was specific to mature oligodendrocytes ($O1^+/MBP^+$ cells). In control cultures approximately 60% of the GFP^+ cells belonged to the oligodendrocyte lineage and this was reduced to approximately 40% after CID treatment. While the relative proportion on $A2B5^+$ and $O4^+$ cells were not altered there was a significant reduction in $O1^+$ and MBP^+ cells. Note that not all $O1^+$ cells express MBP and only those that do (approx 50%) were lost following CID treatment. Data represent the mean+/− standard error from cell counts taken from 3 independently treated coverslips from 2 cell preparations. Scale bar = 25 μm. $p < 0.05$.

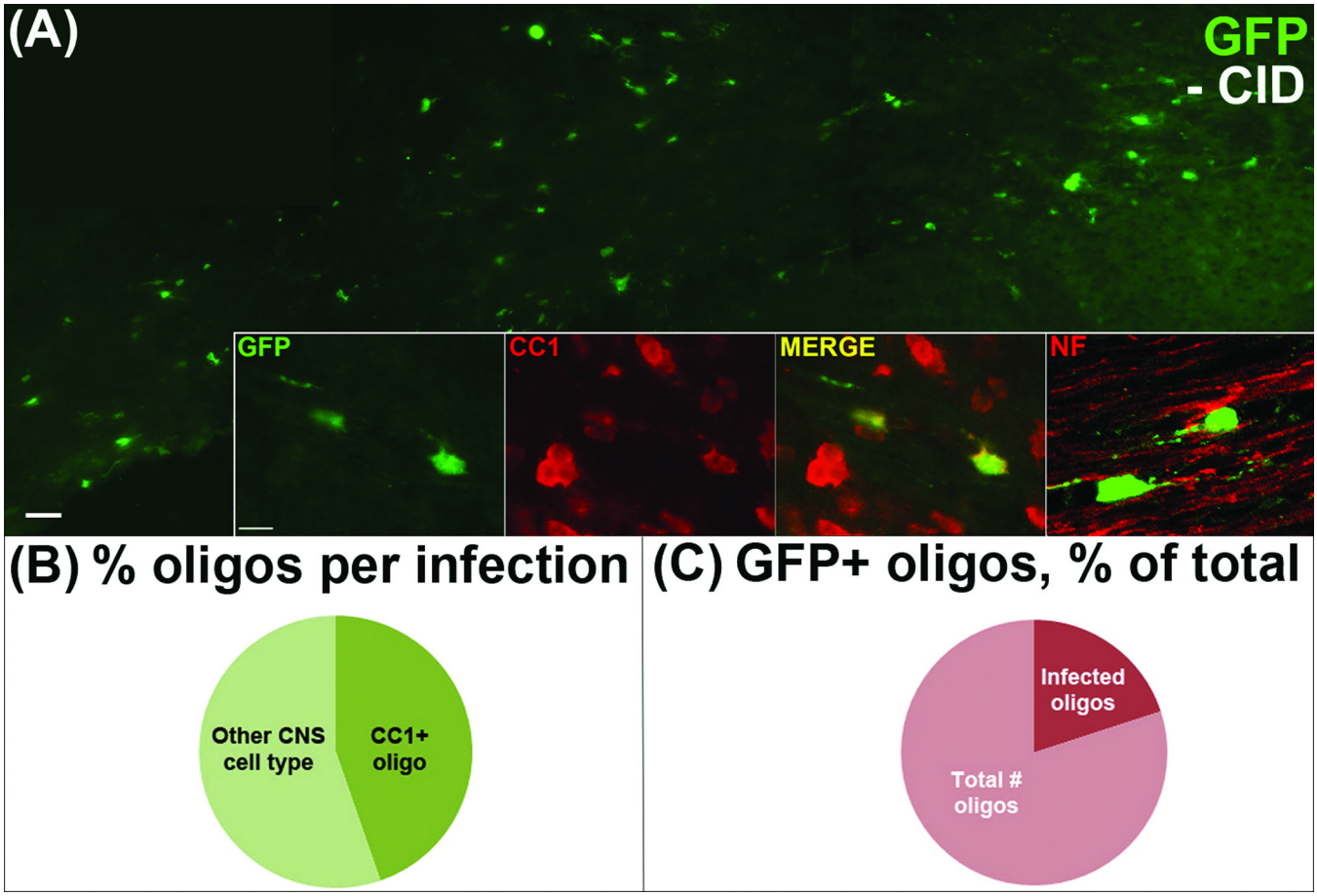

Figure 3.

Localized delivery of lentivirus resulted in robust transfection and gene expression as visualized by GFP expression. (**A**) Representative image of the extent of lentiviral transfection one week after stereotaxically-guided lentiviral injections into the adult rat corpus callosum. Inset demonstrates the effective transduction of mature, $CC1^+$ oligodendrocytes. Confocal analysis of GFP and anti-neurofilament labeling (NF) demonstrated axons myelinated by GFP^+ oligodendrocytes. (**B-C**) Quantitation of the relative proportions of oligodendrocyte lineage cells within the GFP population before CID delivery. Prior to CID injection, $CC1^+$ oligodendrocytes constituted approximately 44% of all cells virally transduced, which represents approximately one quarter of the total number of oligodendrocytes in a given region of corpus callosum. Scale bar = 25 μm. $p < 0.05$.

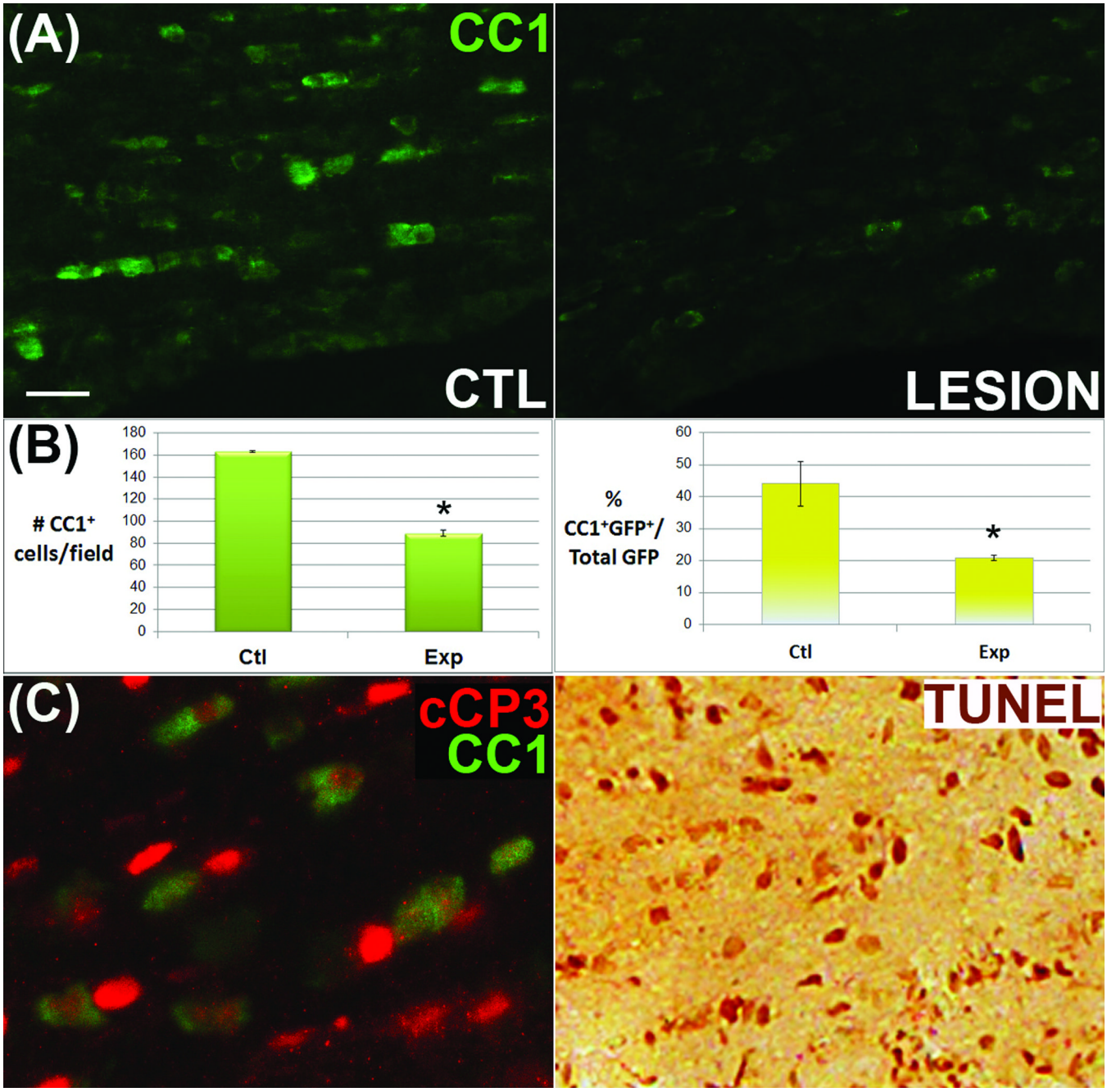

Figure 4.

Injection of CID induced the apoptosis of iCP9 expressing oligodendrocytes in vivo. One week after lentiviral injection into the corpus callosum of adult rats, CID was injected distally into the ipsilateral ventricle to activate iCP9-triggered apoptosis. (**A**) One day post-CID, there was a significant decrease in the number of $GFP^+/CC1^+$ oligodendrocytes compared with either the contralateral hemisphere or to vehicletreated controls. (**B**) Quantitation and comparison of the reduction of CC1+ cells and relative proportion of GFP+ cells expressing CC1. The total number of CC1+ cells was reduced by approximately 50% after CID exposure. Likewise the proportion of GFP+ cells that express CC1 was reduced by approximately 50% after CID treatment. (**C**) Double labeling with cleaved caspase 3 and

CC1 as well as TUNEL labeling confirmed the induction of apoptosis following CID exposure. Scale bar = 25 μm. $p < 0.05$.

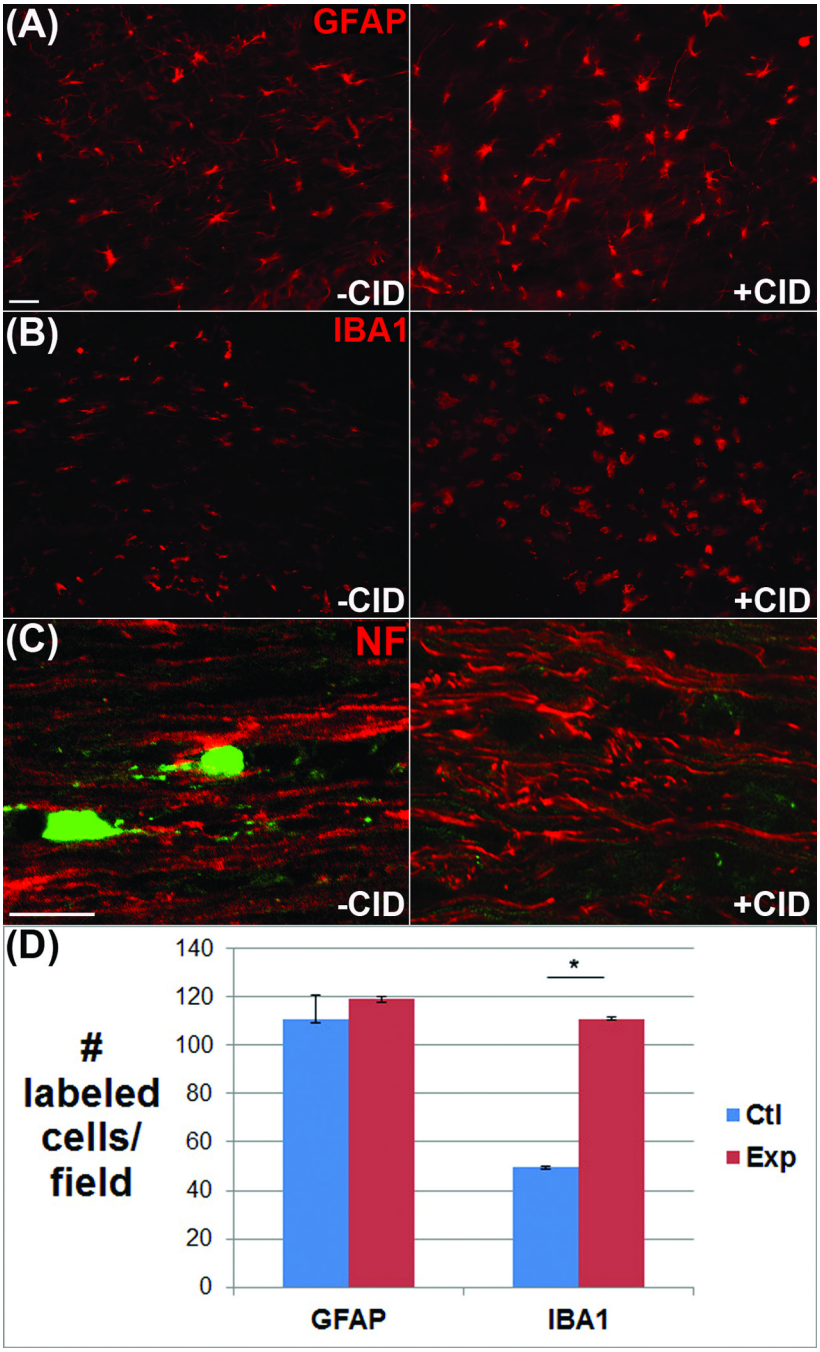

Figure 5.

Injection of CID resulted in selective loss of mature oligodendrocytes in areas of viral transfection. (**A**) Labeling of infected areas with antibodies to GFAP to identify astrocytes demonstrated no significant reduction in GFAP+ cells. (**B-C**) Likewise, IBA1^{+} microglia and NF^{+} axonal neurofilaments were present throughout the transfected area (**D**) Quantitation shows similar numbers of GFAP+ astrocytes +/− CID but a significant increase in microglia. Scale bar = 25 μm. $p < 0.05$.

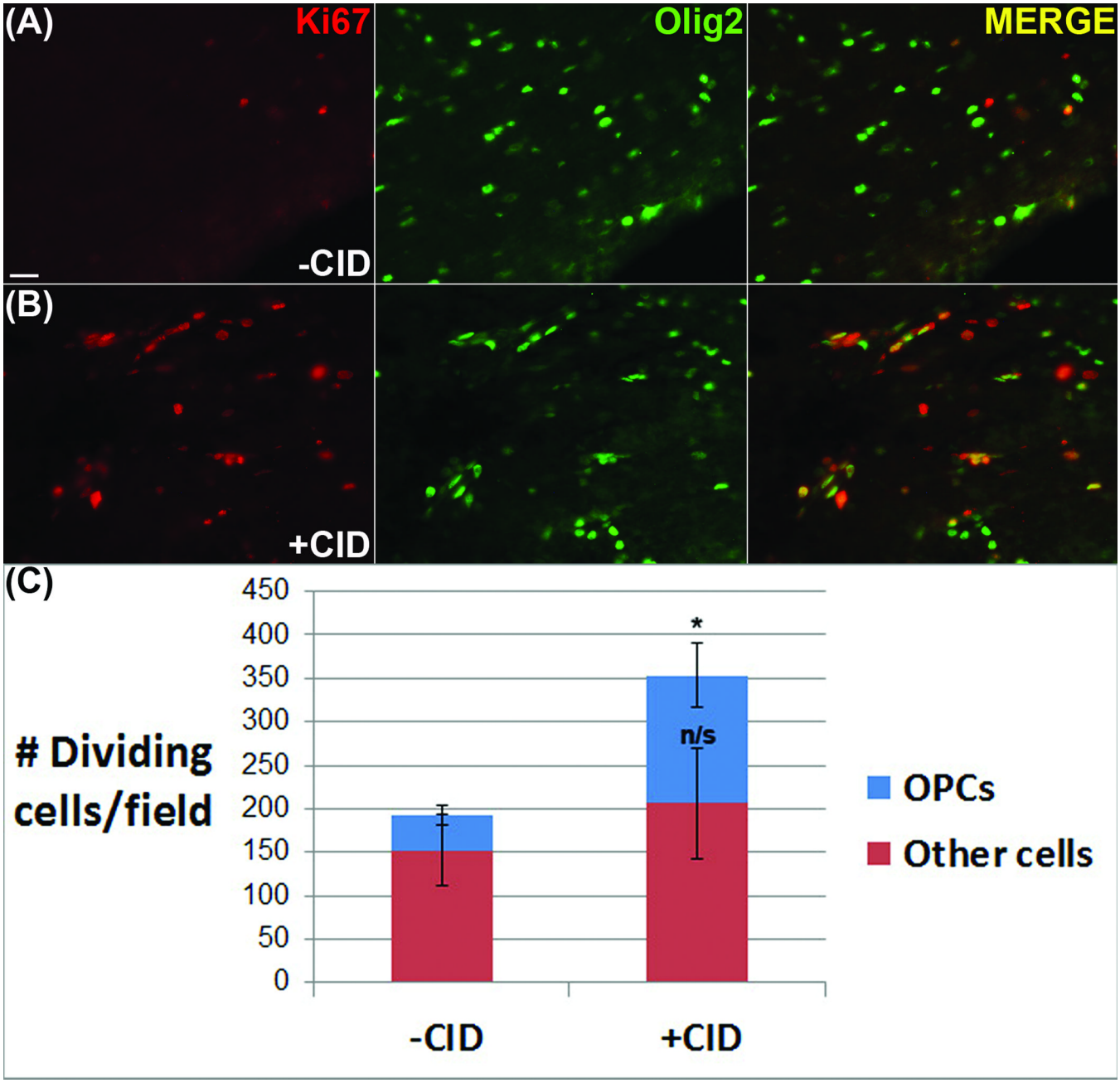

Figure 6.

Oligodendrocyte death increased the number of proliferating OPCs. (**A**) In vehicle-injected control animals, a low level of proliferation ($Ki67^+$) was present in virally-infected regions. (**B**) The level of cell proliferation was markedly increased in animals that received CID injections. Double-labeling Ki67 with an oligodendrocyte lineage marker (Olig2) indicates an increase in the number of proliferative cells which was significant only in the $Olig2^+$ cell population (**C**). Scale bar = 25 μm. $p < 0.05$.

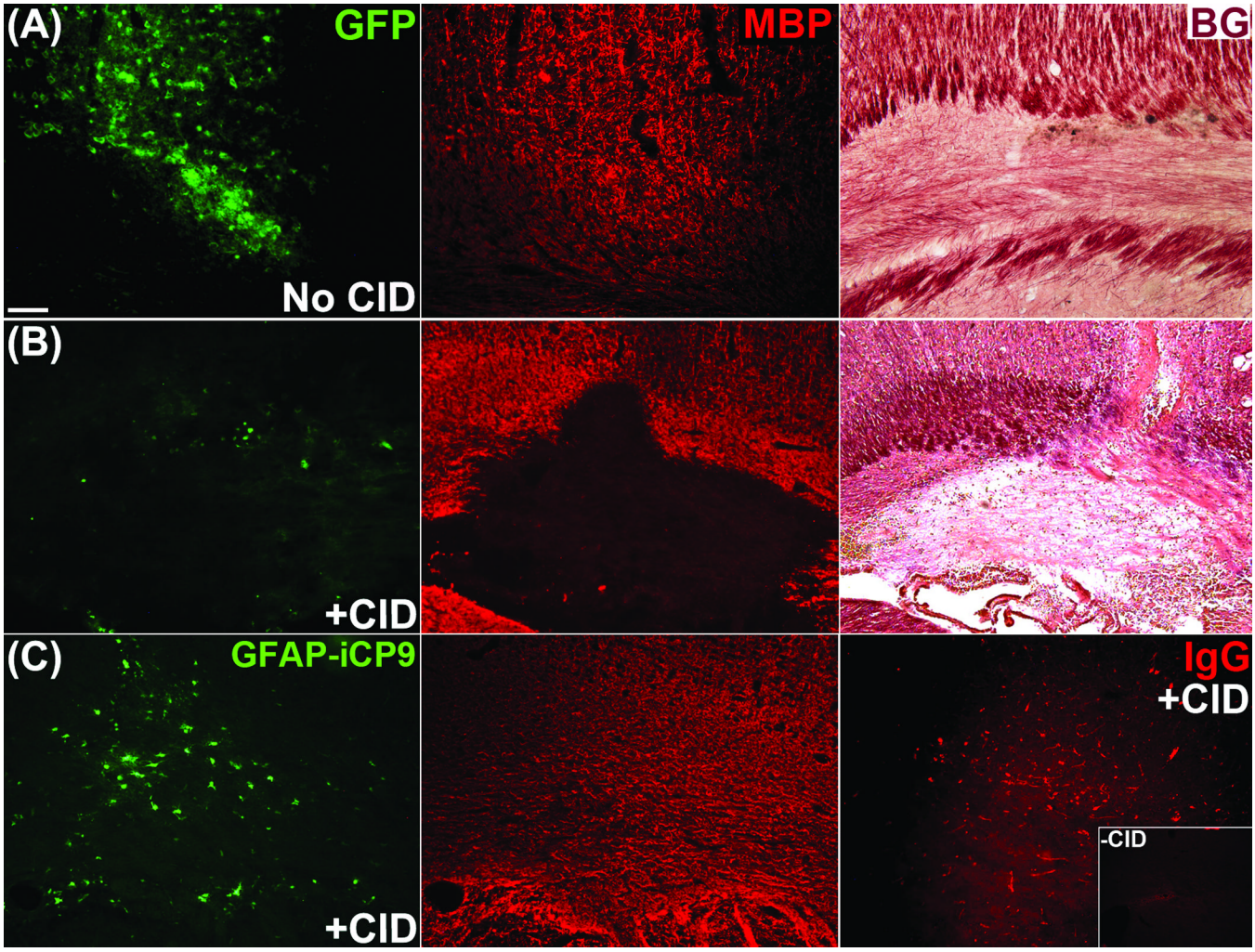

Figure 7.

Oligodendrocyte apoptosis led to rapid myelin loss. (**A**) Myelin perturbation was absent in vehicle-treated control animals, whereas (**B**) CID-treated animals displayed a loss of MBP immunofluorescence as well as Black Gold signal. (**C**) Control experiments demonstrated that demyelination was not attributable to either virus or CID alone as parallel studies using a separate viral construct to target $GFAP^{+}$ astrocytes lacked myelin loss despite functional evidence of astrocyte loss using a blood-brain-barrier IgG assay. Scale bar = 50 μm. $p < 0.05$.

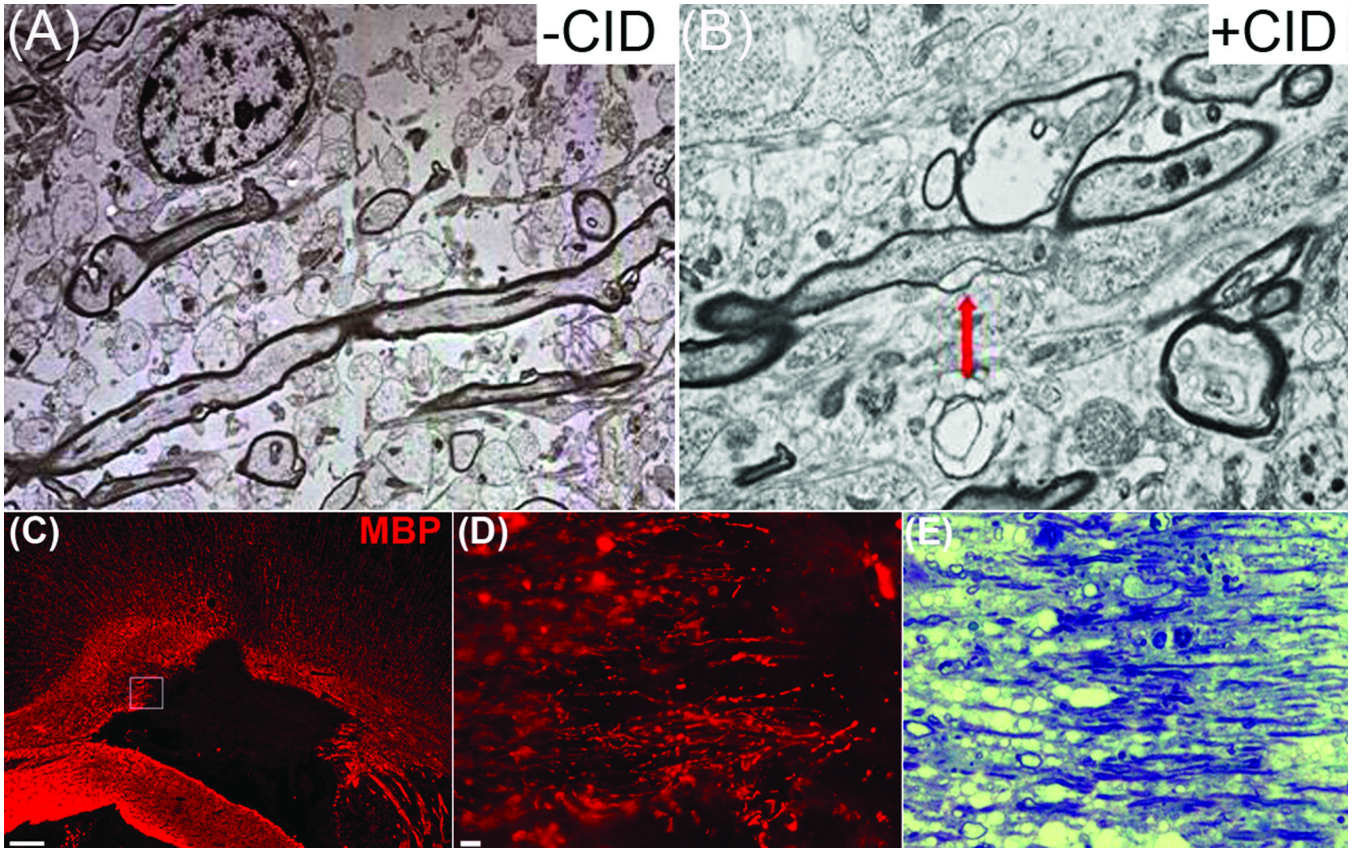

Figure 8.

Electron microscopy revealed demyelination of intact longitudinal axons in CID-treated rats expressing MBP-iCP9. (**A-B**) Consistent with the loss of oligodendrocytes, demyelinated axons were present in CID-treated but not control animals. Demyelination invariably began at could at nodes of Ranvier (arrow) resulting in areas of internodal demyelination. (**C-D**) The borders of apoptotic lesions contained layers of preserved and degraded myelin, seen by (**D**) MBP immunolabeling and confirmed by thin-sections stained with Toluidine Blue (**E**). Scale bar = (C) 50 μm; (D) 25 μm.

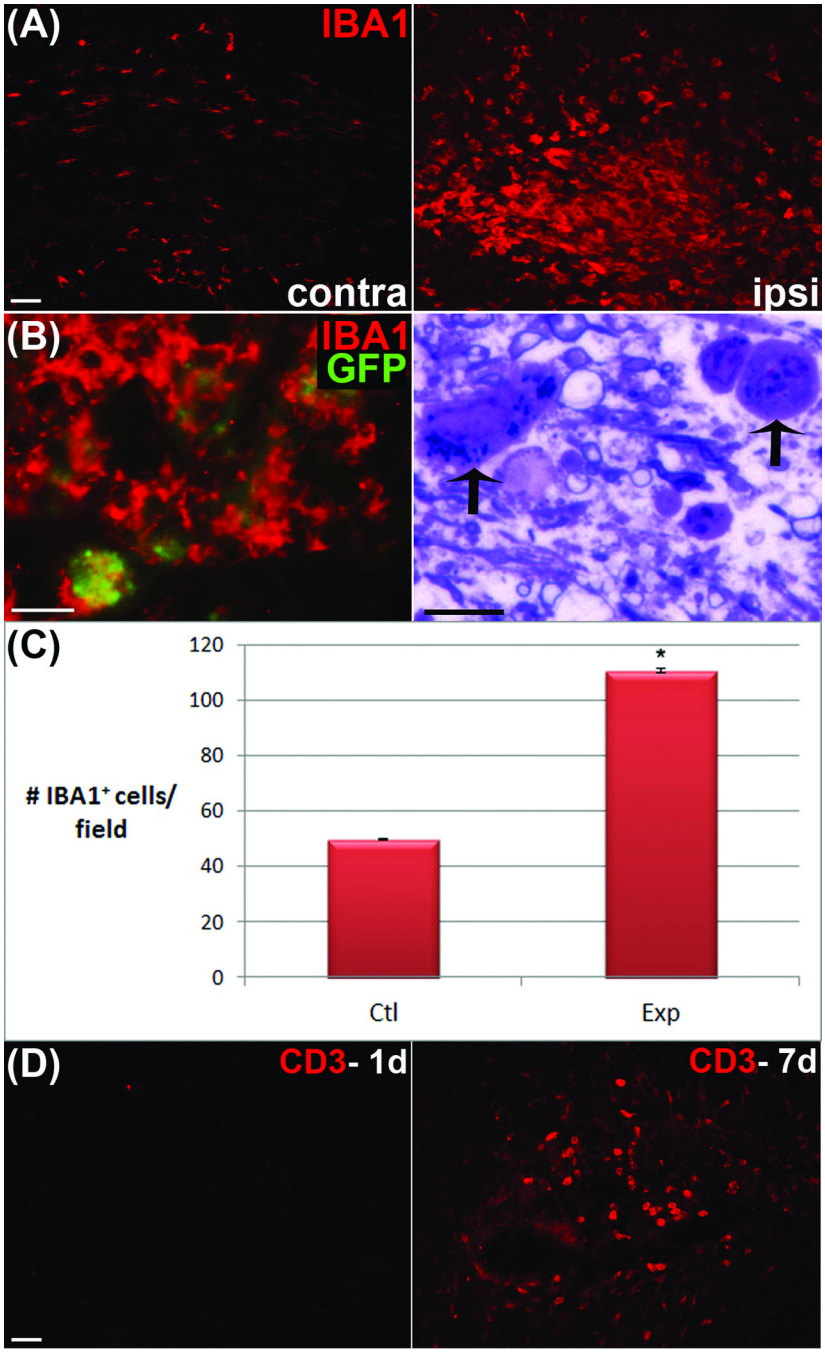

Figure 9.

A robust, highly-localized microglial response accompanied CID-mediated demyelination. (**A**) IBA1$^+$ microglia/macrophages on the contralateral side of an experimental animal exemplify the basal, ramified morphological state whereas on the ipsilateral injection side, microglia display activated, amoeboid morphology. (**B**) Co-localization of GFP$^+$ fragments with IBA1 and thin sections stained with Toludine Blue suggest phagocytosis by activated microglia. (**C**) Quantitation of increases in IBA1+ cells following CID induced oligodendrocyte apoptosis (**D**) Extensive T-cell infiltration as shown by anti-CD3 staining

was limited twenty-four hours after CID treatment but increased at 7 days post demyelination. Scale bars = 25 μm; $p < 0.05$.